



# Nationwide Demand Modeling for an Urban Air Mobility Commuting Mission

Mark T. Kotwicz Heniczek\*<sup>✉</sup> and Brian J. German<sup>†</sup>  
*Georgia Institute of Technology, Atlanta, Georgia 30332*

<https://doi.org/10.2514/1.D0371>

In this paper, we present a comprehensive and reproducible urban air mobility (UAM) demand model centered around publicly available data and open source tools capable of demand estimation at the national level. A discrete mode-choice demand model is developed using longitudinal origin–destination employment statistics flow data, American community survey economic data, and the Open Source Routing Machine (OSRM) to identify the utility of a UAM commuter service relative to other modes of transportation. Using the implemented model, we identify New York City, San Francisco, and Los Angeles as cities with the highest potential commuter demand, and Seattle as the city most resilient to increases in delay time. A sensitivity study of demand is performed and shows that strong demand exists for short trips with low total delay times and for longer trips with a low ticket price per kilometer, with the former showing resilience to increases in operational costs and the latter showing resilience to increases in delays. The demand model is supported by a speed-flow model, which fuses highway performance monitoring system data with OpenStreetMap data to provide traffic-adjusted road segment speeds to OSRM. The speed-flow model has the capability of providing congestion data for road segments across the United States without the use of commercial data sets or routing services and is shown to improve routing duration accuracy in congested regions.

## I. Introduction

DEMAND modeling is key to estimating the feasibility and scalability of transportation services such as urban air mobility (UAM). A number of qualitative and quantitative methods exist for modeling transportation demand, including surveys, time-series methods, econometric methods, and artificial intelligence methods [1]. First applied in the 1950s, the four-step model (FSM) remains a popular econometric approach for estimating demand of a specific transportation mode [2]. FSM, as the name suggests, generally consists of four steps: 1) trip generation, which seeks to estimate the total number of trips with origins or destinations within a given area of interest; 2) trip distribution, which allocates the number of trips for each origin–destination (OD) pair in the area; 3) mode choice, which models the probability of utilization of each mode of transportation for each OD pair; and lastly 4) route assignment, which determines the specific route followed by an individual to reach their destination. Mode choice models are motivated by the concept of utility maximization—that individuals tend to choose the mode of transportation that provides the highest possible utility. Mode choice models and other aspects of demand modeling gained traction within the aviation transportation sector as airline competition increased after deregulation [1,3].

More recently, demand modeling of potential UAM transportation services has become a topic of interest for many researchers due to the significant investments, market size claims, and media exposure that UAM has received [4–6]. Booz Allen Hamilton, for example, published a report that projected a near-term annual market value for UAM services of \$2.5 billion and an unconstrained market (ignoring infrastructure, capacity, public acceptance, and weather constraints) value of \$500 billion annually [4].

Prior studies in UAM demand modeling have employed a variety of approaches due to untested nature of UAM as a transportation mode, for which customer behavior, vehicle performance, and oper-

ating costs are not yet known. Several authors used mode choice models to characterize demand. Syed et al. applied a conditional logit model to census data to estimate on-demand commuter demand in the San Francisco and Washington, DC, areas [7]. Ploetner et al. derived an incremental logit model to simulate demand for UAM transportation services [8]. Rimjha and Trani applied a mixed conditional logit demand model to data from the 2019 Los Angeles International Airport Passenger Survey to estimate demand for a UAM airport shuttle service [9]. Wu and Zhang used Tampa Bay regional planning model data and a deterministic integer programming approach to estimate demand for a UAM commuting service [10]. Justin et al. utilized a multinomial logit model to estimate demand for a regional air mobility service based on the National Long Distance Passenger Origin Destination data set published by the Federal Highway Administration [11]. Haan et al. provided a ranking of the 40 cities in the United States most suitable for UAM operations by applying a multinomial logit model to cell phone location data and census income data, calibrated with a stated preference survey data [12]. Lastly, Straubinger et al. developed a general equilibrium model to explore the welfare impact of UAM operations on a distributed population [13].

Several studies focused on leveraging public databases to quantify regional or national demand. Kotwicz Heniczek et al. used census data to explore nationwide and regional demand potential for near-term UAM operations based on income and time savings of a UAM service relative to ground transportation [14]. Bulusu et al. estimated commuter demand based on time savings relative to existing ground transportation using data from the San Francisco County transportation authority [15]. Lastly, Alvarez et al. leveraged the New York taxi database to approximate demand based on fractional replacement of taxi services [16]. Multiple authors also conducted stated-preference surveys to aid prediction of demand of UAM, namely, Garrow et al. [17–19], Fu et al. [20], and Al Haddad et al. [21].

In this paper, we make use of a simplified FSM and extend previous efforts [14,22] to form a scalable traffic and demand estimation methodology that requires only publicly available data and tools. This work provides a more comprehensive, reproducible, and more scalable demand modeling framework for UAM commuting operations than currently exists in the literature.

## II. Overall Methodology

The demand estimation model implemented in this work uses commuter flow data as a basis for the first two steps of the FSM, trip generation and trip distribution. Applying commuter flow data in

Received 14 February 2023; revision received 14 July 2023; accepted for publication 15 July 2023; published online 29 September 2023. Copyright © 2023 by Mark T. Kotwicz Heniczek and Brian J. German. Published by the American Institute of Aeronautics and Astronautics, Inc., with permission. All requests for copying and permission to reprint should be submitted to CCC at www.copyright.com; employ the eISSN 2380-9450 to initiate your request. See also AIAA Rights and Permissions www.aiaa.org/randp.

\*Research Engineer II, Daniel Guggenheim School of Aerospace Engineering; mark.kotwicz@gatech.edu. Student Member AIAA.

<sup>†</sup>Associate Professor, Daniel Guggenheim School of Aerospace Engineering; Associate Fellow AIAA.

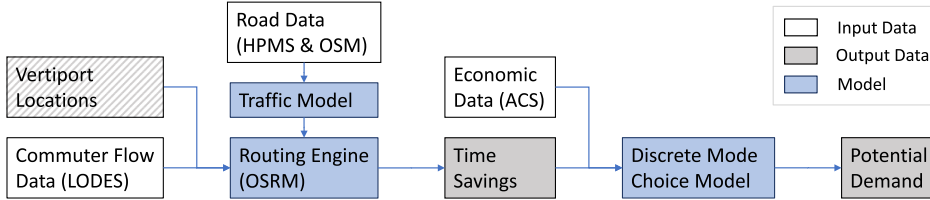


Fig. 1 Demand methodology flowchart.

this context is possible because the data provide both the residence and the place of work of commuters and therefore provide the origin and destination (or vice versa, depending on time of day) for all commuting trips in a given area. Mode choice (step 3 of FSM) is performed using a discrete choice model based on utility maximization between a UAM commuting service relative to alternative (ground-based) modes of transportation. Lastly, trip allocation (the last step of FSM) utilizes a speed-flow congestion model in conjunction with a ground vehicle routing engine to obtain minimum-time multimodal trajectories. A breakdown of the demand model methodology is provided in Fig. 1. Note that *vertiport locations* are hatched in gray in Fig. 1 because they can also be an output if the demand model is used as a part of a vertiport optimization framework.

### III. Commuting and Economic Data Sources

Five publicly available data products are used by the demand model: 1) Longitudinal Employer-Household Dynamics (LEHD) Origin-Destination Employment Statistics (LODES) data [23]; 2) American Community Survey (ACS) commuting and workplace data [24]; 3) Topologically Integrated Geographic Encoding and Referencing (TIGER) block data [25]; 4) Highway Performance Monitoring System (HPMS) road utilization data; and 5) OpenStreetMap (OSM) geographic road data. More specifically, 2019 block-group-level Longitudinal Employer-Household Dynamics Origin-Destination Employment Statistics (LODES) data are used to obtain the residential and workplace locations, and 2019 tract-level ACS data (Table S1902) are used to obtain the mean income and income distribution of individuals across the United States. TIGER block data, on the other hand, are used to correlate census block identification numbers to geographic boundaries and to calculate geographic coordinates of tract centroids.

Together, the LODES, ACS, and TIGER data sets provide the origin (home) and destination (work) location, and the approximate income of each commuter in a given region. Vertiport locations are either chosen based on existing airport and heliport infrastructure, chosen manually, or obtained through optimization, using methods such as  $k$ -means clustering [26,27], genetic algorithms, integer programming [10,28], or combinatorial methods [29]. The vertiport locations, in conjunction with OD locations obtained from the LODES data, are fed to the traffic-informed routing engine to obtain all relevant driving times (between home and the workplace, between home and the nearest vertiport, and between the workplace and the nearest vertiport). Lastly, HPMS and OSM data are used by the traffic model to estimate congestion factors along road segments across the United States. The time savings of using a UAM commuting service, along with commuter economic data obtained from the ACS database, are utilized by the discrete choice model to determine the utility a UAM commuter service relative to car-based commuting.

#### A. Data Limitations

Several factors, in addition to any errors present in the data, limit the accuracy of the data sets being employed. Namely, the LODES data set is based on administrative records, meaning that a company's headquarters location is sometimes erroneously recorded as an individual's workplace address. Similarly, those who work from home may be registered as working at the company's address rather than from home. The LODES data are also generalized from the block

level to the block-group level to reduce the size of the data set, with origins and destinations assumed to be located at the centroids of each block group. Given the relatively small land area of block groups, this generalization is not expected to have a meaningful impact on demand estimation.

Economic data accuracy, on the other hand, is primarily limited by three factors: 1) LODES data are utilized at the block-group level but the ACS data of interest (Table S1902) are available only at a tract level; 2) ACS data are tied only to residential location, meaning that no differentiation is made for individuals who live within the same tract but work in different areas of a city; and 3) the ACS income distribution data are binned in increments of \$5,000 to \$50,000 and do not provide granularity past \$200,000.

To address the aforementioned data limitations, several assumptions are made regarding the income distribution of residents within tracts: 1) income is assumed to be evenly distributed within block groups of the same tract to bridge the resolution discrepancy between ACS and LODES data, 2) the residential location (origin tract) is used to associate income to each OD pair, and 3) the income is assumed to be uniformly distributed within binned increments and the income distribution past \$200,000 is approximated using Pareto's power law.

Data accuracy is also limited by the long update cycles of the government data products used in this work. Specifically, ACS data are released every two years and releases are delayed by one year. The LODES data are released every year but is currently delayed by three years. Likewise, HPMS data are released every year but delayed by several years. The aforementioned data sets could potentially be scaled using additional more current sources of information, such as yearly regional population data but such efforts were not pursued in this work.

#### B. High-Earner Income Distribution Estimation

Since early users of UAM services are likely to be high earners due to the elevated cost compared to ground transportation [4], a model is necessary to estimate the income distribution above \$200,000. This distribution is estimated using Pareto's power law, which has been shown in the literature to represent the long tail of the high-income distribution [30–32]. The cumulative distribution function of a Pareto curve can be reformulated into Pareto's law, given in Eq. (1), that defines the number of individuals,  $N_x$ , who have an annual income of at least  $x$ :

$$N_x = \beta x^{-\alpha} \quad (1)$$

where  $\beta$  and  $\alpha$  are the scale and shape coefficients that define the distribution. These coefficients can be directly calculated because the mean value of a Pareto distribution with a minimum value,  $x_m$ , of 200,000, assuming  $\alpha > 1$ , is known to be

$$\bar{x}_h = \frac{\alpha x_m}{\alpha - 1} \quad (2)$$

Although  $\bar{x}_h$ , the mean income of high earners (individuals earning at least \$200,000), is not known, we can relate it to the mean of the full income distribution,  $\bar{x}$ , which is known:

$$\bar{x} = \frac{N_h \bar{x}_h + \sum_{x=0}^{200,000} N_x x}{N_0} \quad (3)$$

Rearranging Eq. (3) to solve for  $\bar{x}_h$ , we obtain

$$\bar{x}_h = \frac{\bar{x}N_0 - \sum_{x=0}^{200,000} N_x x}{N_h} \quad (4)$$

Combining Eqs. (1), (2), and (4) we have three equations and three unknowns, and we can numerically solve for the coefficients  $\beta$  and  $\alpha$  as

$$\alpha = \frac{\bar{x}_h}{\bar{x}_h - x_m} \quad (5)$$

$$\beta = N_h x_m^\alpha \quad (6)$$

The mean income  $\bar{x}$ , total population  $N_0$ , number of individuals that earn above \$200,000 ( $N_h$ ), and the income distribution up to \$200,000 are obtained from Table S1902 of the ACS data.

#### IV. Vehicle Routing and Congestion Model

Routing of UAM vehicles in the near future is anticipated to be segregated from large commercial air traffic and be restricted to a corridor structure, within which vehicles operate under UAM specific rules, procedures, and performance requirements [33,34]. Given that the corridor structure may follow existing helicopter routes or ground road infrastructure and will need to avoid airspace restrictions, consider community noise regulations, and avoid weather events, UAM vehicle routes between vertiports are unlikely to be a straight line [35,36].

In this work, however, since corridor structures have not yet been defined for any region, we assume that UAM flights follow a direct route but include a term to account for routing delays and detours. Flight duration is therefore modeled to be a function only of the Euclidean distance between two vertiports ( $d_{e,V_O \rightarrow V_D}$ ), the vehicle cruise speed ( $v_e$ ), and a delay term ( $t_{\text{delay}}$ ), as shown in Eq. (7). The delay term accounts for any additional time required for passenger enplanement and deplanement, routing detours, and for differences in forward speed during takeoff, cruise-climb, descent, and landing relative to the cruise speed. In the nationwide demand results presented in the paper, vertiport locations are assumed to coincide with the origin and destination of a given trip, and the delay term is also used to account for additional time to drive to the vertiport from home and from vertiport to work or vice versa. These simplifications allow for rapid first-order approximations for potential demand and are consistent with the level of abstraction of the presented work. Given the number of uncertainties associated with UAM services, use of a straight-line model is not expected to have a measurable impact on our results.

$$t_{e,V_O \rightarrow V_D} = \frac{d_{e,V_O \rightarrow V_D}}{v_e} + t_{\text{delay}} \quad (7)$$

Ground vehicle routing is also necessary to provide accurate estimates of time savings for a UAM commuting service given its multimodal nature. In particular, accurate drive-time estimates are needed between OD pairs, as well as between vertiports and origins and vertiports and destinations. Due to the large quantity of routing calls necessary (the city of Atlanta on its own, e.g., requires several million routing calls), commercial routing services such as the Google Distance Matrix Application Programming Interface (API) are computationally and financially expensive.

Consequently, the Open Source Routing Machine (OSRM) engine [37] was selected to find minimum duration paths for road networks, which has two major advantages compared to a commercial routing service: 1) unlimited and free API calls and 2) the ability to download the source code and required mapping files to a local directory, significantly increasing the speed of routing queries. A notable disadvantage of using OSRM for routing, however, is the lack of consideration of traffic congestion data. Several traffic estimation methods were considered in an attempt to introduce traffic data into

the ground vehicle routing engine in a reliable and cost-effective manner. Each method used OSRM as the main routing engine but differed in the manner in which traffic was applied to route duration estimates.

Firstly, commercial traffic products were used to inform a reduced road-network graph, and graph traversal methods were used to obtain a congestion factor for any given OD pair in the graph. Although this methodology yielded promising results, it was not implemented due to restrictive or unclear terms of service agreements present with many commercial routing and traffic services.

Secondly, ACS commuting duration data were used to generate individual traffic factors at the OD pair and at the tract level. The congestion factors were obtained by minimizing the error between the OSRM-based LODES commuting data and the ACS commuting data. The ACS commuting data, however, suffer from the same limitations to ACS economic data; i.e., the provided commute duration distribution is coarsely binned and is only tied to the residential tract, making it difficult to apply the distributions to OD pairs. Although error minimization between the two data sets could work in theory, inconsistencies between the LODES and ACS data sets, coupled with the limitations of the ACS data, rendered the method inaccurate and inconsistent.

Next, we tried taking advantage of congestion databases available online that provide traffic speeds or congestion indices at a citywide level for all major metropolitan areas in the United States. We implemented a simple lookup function that checked if a metropolitan area with a known congestion factor exists, and scaled that congestion factor based on the perpendicular distance between the OD pair and that city center. Although quite trivial in its implementation, the method did improve OSRM route duration estimates relative to commercial traffic engines such as Google Maps and Bing Maps.

Finally, the HPMS data set, a public national database on road characteristics and utilization, was leveraged to estimate congestion factors using a speed-flow model. The HPMS approach was found to be the most reliable and accurate method to introduce traffic data into the demand model and was used to generate the demand estimates presented in this paper. Details regarding the implementation of the speed-flow model are presented in more detail in the subsequent sections.

##### A. Speed-Flow Congestion Model

Speed-flow models that adjust the free flow speed (FFS) based on road characteristics and flow rate are well established in the literature [38–41]. The speed-flow models described in Volumes 2 and 3 of the *Highway Capacity Manual* [40,42] were selected due to their simplicity, lack of tuning parameters, and compatibility with data from the Highway Performance Monitoring System (HPMS) database. More accurate or complex models exist; however, they typically contain parameters that require calibration [43,44] or include time as a dependent variable [45,46].

The HPMS is a public, federal database that provides information on the extent, condition, performance, use, and operating characteristics of highways within the United States [47]. A subset of the reported parameters in the HPMS data set, referred to as full extent data items, is reported for the full extent of the system network, including all National Highway System (NHS) routes, principal arterial, minor arterial, major collector, and urban minor collector roads.

Although a direct measure of congestion is not provided within the HPMS data set, the annual average daily traffic (AADT) and number of through lanes are both provided as full extent data items and can be used to adjust the FFS of highway segments. Together, AADT and the number of lanes can be used to obtain the number of vehicles per lane per day for any road segment within the data set. To estimate the demand flow rate during peak traffic conditions, however, we need to convert average daily flow to directional, peak hourly flow  $v_p$  as described by Eq. (8).

$$v_p = \frac{\text{AADT} \cdot K \cdot D_{\text{traffic}}}{N_{\text{lanes}}} \quad (8)$$

where  $K$  is the proportion of daily traffic occurring during the peak hour of the day,  $D$  is the proportion of traffic in the peak direction during the peak hour of the day, and  $N_{lanes}$  is the number of lanes designed for through-traffic for a given direction of travel [40]. Flow factors  $K$  and  $D$  were assumed to have values of 0.10 and 0.55, typical of rural and urban freeways [40], respectively, due to their limited availability within the HPMS data.

The freeway speed-flow model described by Eqs. (9a–9e), provided in Volume 2 of the *Highway Capacity Manual* [40], describes uninterrupted traffic flow speed  $S$  as a function of FFS, and the peak hourly flow  $v_p$ . It should be noted, however, that several modifications have been made to the model to extend its applicability on a national scale. First, the limits have been removed on the maximum speed of Eq. (9a) to extend the model to highways with posted speeds of 80 and 85 mph. Secondly, to accommodate this extrapolation, Eqs. (9a–9e) have been modified so that FFS remains a variable in the equations rather than a fixed value, meaning that an FFS of 80 mph would read  $80 - 0.00001107(v_p - 1,000)^2$  rather than  $75 - 0.00001107(v_p - 1,000)^2$ .

$$S(FFS, v_p) = \begin{cases} FFS - 0.00001107(v_p - 1,000)^2, & \text{if } v_p > 1,000 \text{ and } 72.5 \geq FFS \\ FFS - 0.00001160(v_p - 1,200)^2, & \text{if } v_p > 1,200 \text{ and } 67.5 \geq FFS < 72.5 \\ FFS - 0.00001418(v_p - 1,400)^2, & \text{if } v_p > 1,400 \text{ and } 62.5 \geq FFS < 67.5 \\ FFS - 0.00001816(v_p - 1,600)^2, & \text{if } v_p > 1,600 \text{ and } 57.5 \geq FFS < 62.5 \\ FFS - 0.00002469(v_p - 1,800)^2, & \text{if } v_p > 1,800 \text{ and } 52.5 \geq FFS < 57.5 \\ \frac{1}{2} FFS \cdot \left(1 + \left(1 - \frac{v_p}{52.8 \cdot FFS}\right)^{0.21}\right), & \text{otherwise} \end{cases}$$

Thirdly, Eq. (9) has been assumed to function in a portion of the congested regime, up until a congestion factor  $C_F$  of 0.5 is reached [as shown in Eq. (10)], which corresponds to a volume-to-capacity ratio of approximately 1.2. This approximation is expected to lead to an overprediction of speed for congested road segments due to the omission of queuing and propagation effects, but higher fidelity approaches typically require temporal data or tuning parameters and were deemed out of scope for this work.

$$C_F = \max\left(0.5, \frac{S}{FFS}\right) \quad (10)$$

Equation (9e) is not extended to slower speeds because roads with posted speeds of 50 mph and below tend to experience interrupted

flow (signal controlled), which are not well-characterized by a freeway speed-flow model. Instead, congestion is crudely approximated at these lower speeds using the proximity adjustment factor given by Eq. (9f) and defined in Volume 3 of the *Highway Capacity Manual* [42], which adjusts free flow time for the effect of traffic density.

Lastly, FFS was assumed to coincide with posted speed limits along road segments (obtained from OSM data if missing from the HPMS data set). With this assumption and the modifications discussed previously, sufficient information is known to estimate congestion factors for the majority of road segments in the United States. In addition to its use in this paper, the developed traffic estimation methodology can facilitate integration of high-level congestion data into operations research studies by avoiding the need for simulation or commercial traffic data.

### 1. OSM Graph-Edge Matching Validation

Once congestion data have been extracted from the HPMS data set, road segments of the speed-flow model are matched to OSM graph

$$\text{if } v_p > 1,000 \text{ and } 72.5 \geq FFS \quad (9a)$$

$$\text{if } v_p > 1,200 \text{ and } 67.5 \geq FFS < 72.5 \quad (9b)$$

$$\text{if } v_p > 1,400 \text{ and } 62.5 \geq FFS < 67.5 \quad (9c)$$

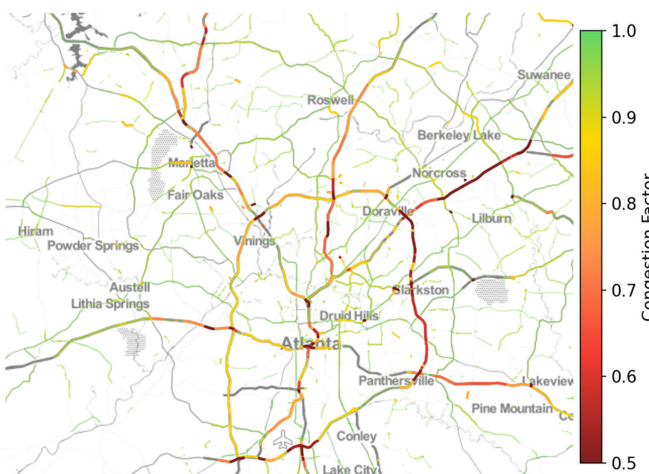
$$\text{if } v_p > 1,600 \text{ and } 57.5 \geq FFS < 62.5 \quad (9d)$$

$$\text{if } v_p > 1,800 \text{ and } 52.5 \geq FFS < 57.5 \quad (9e)$$

$$\text{otherwise} \quad (9f)$$

edges to facilitate integration of congestion data into the demand model. By conflating the two data sets and providing OSRM with congested speed data on associated edges of the graph, OSRM can be used directly to perform traffic-informed routing. We refer to OSRM as Traffic-Informed OSRM (TI-OSRM) when the routing engine is informed by the speed-flow congestion model to facilitate comparison between routing engines in the subsequent sections.

Although sophisticated road geometry conflation methods exist [48], we found that matching graph edges based on distance, lane count, and road orientation was sufficient, as demonstrated in Fig. 2. This was due to the close spatial agreement of edge segments before conflation and the limited number of nearby segments given that only “motorway,” “trunk,” and “primary” roads were considered from the OSM graph. The omission of lesser road types is not expected to have



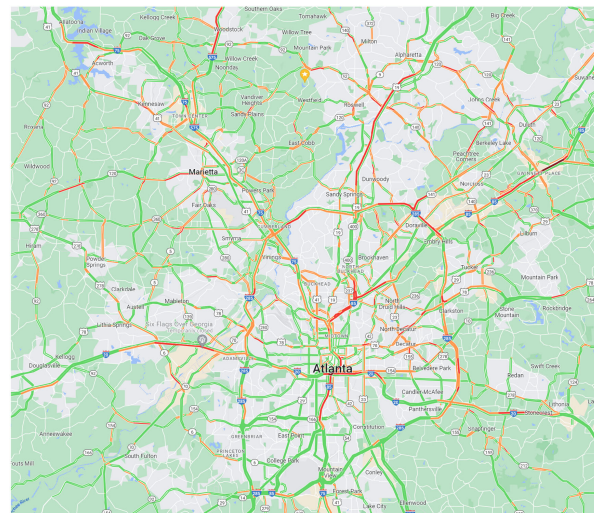
a) Congested segments with geometry from HPMS



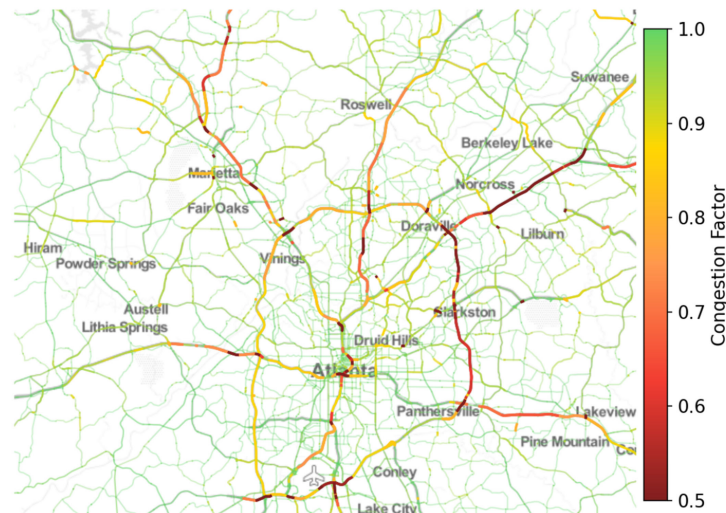
b) Matched OSM segments

Fig. 2 Qualitative comparison of edge-matching accuracy between the HPMS and OSM road network graphs.

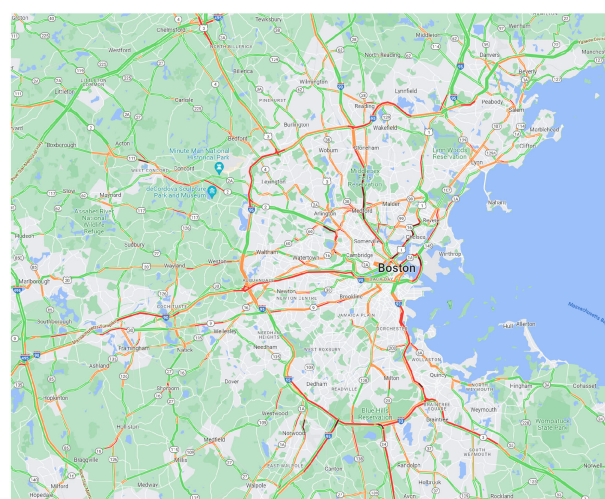
a meaningful impact on the results due to the small number of roads of these types that experience congestion in the implemented speed-flow model, as shown in Figs. 2 and 3.



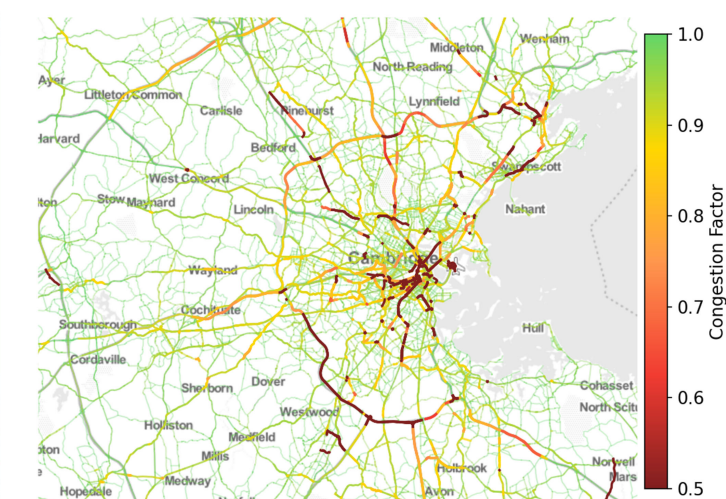
a) Atlanta: map data ©2023 google



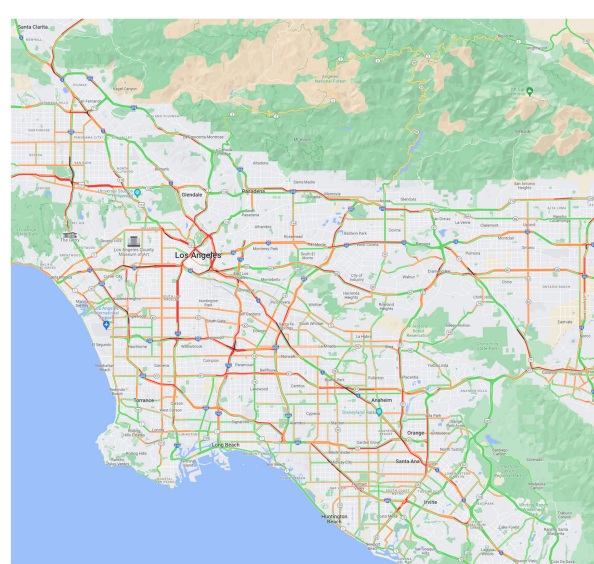
b) Atlanta: speed-flow congestion model



c) Boston: map data ©2023 google



d) Boston: speed-flow congestion model



e) Los angeles: map data ©2023 google



f) Los angeles: speed-flow congestion model

Fig. 3 Qualitative comparison between typical Tuesday traffic at 8:00 a.m. reported by Google Maps and the congestion factor estimated using the implemented speed-flow congestion model.

first qualitatively compared to congestion reported by Google Maps for the cities of Atlanta, Seattle, and Los Angeles. These qualitative results are illustrated in Fig. 3. Google Map traffic results were kept within the Google Maps environment to avoid possible terms of service violations. Unfortunately, differences in map styles hinder comparison between the two sets of maps. Nevertheless, good agreement can be observed for the majority of highway and interstate segments.

Note that the speed-flow model is representative of a generic peak hour of traffic, whereas Google Map traffic data are specific to “typical” Tuesday 8:00 a.m. traffic, which accounts for some of the congestion discrepancies in Fig. 3. It is likely possible to improve the performance of the speed-flow model by tuning its parameters, particularly for smaller urban roads or if the model were limited to a specific city; however, our goal in the present paper is to develop a method suitable for nationwide results, and therefore we did not examine limiting or tuning the model to specific regions.

### 3. Speed-Flow Model Validation

Validation of the speed-flow model was performed by selecting a random subset of 1000 OD pairs from the LODES data set in the vicinity of several major cities in the United States and comparing routing results between several routing engines: OSRM, TI-OSRM, and the Bing and Google Map routing engines. Route distance and duration without traffic estimates are first compared to explore possible limitations and sources of error in the routing engines.

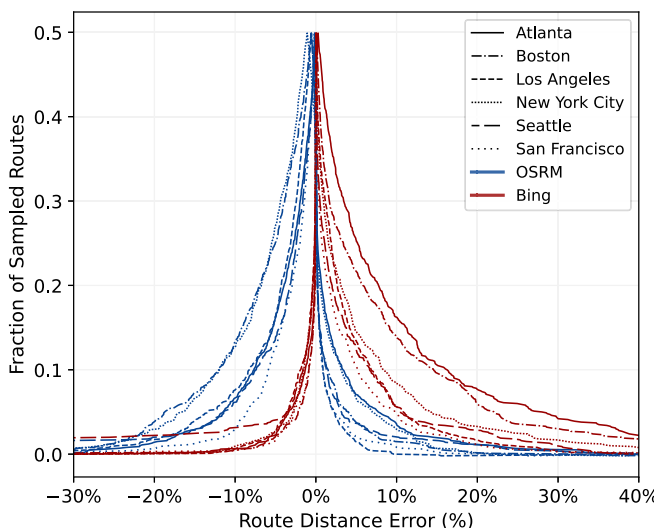
Figure 4a illustrates the folded cumulative distribution function (CDF) of error of the distance estimates obtained with the OSRM and Bing routing engines relative to estimates obtained using the Google Maps routing engine. Use of a folded CDF (where the distribution is folded at the median such that the plotted function is  $p$  when  $p < 0.5$  and  $1 - p$  otherwise) facilitates comparison of the performance of each routing engine, particularly enabling comparison of the median, skew, range, and percentiles of each distribution. For example, we can see that the medians of the distributions in Fig. 4a are centered on zero, whereas the medians are more scattered in Fig. 4b. More specifically, looking at OSRM route duration error in New York City (NYC), represented by a densely dotted blue line in Fig. 4b, we can read that NYC routes have a median error of  $-4\%$ , and that 7% of NYC routes have error below  $-20\%$ , whereas only 1% of routes have error above  $20\%$ , meaning that 92% of routes in NYC have a duration error between  $-20$  and  $20\%$  relative to Google Maps.

Revisiting Fig. 4a, we can observe that distance estimates generally showed good agreement, with approximately 85% of routes obtained with Bing and OSRM remaining within 10% of the Google

Maps distance estimate. Both OSRM and Bing have a median error near zero; however, we can observe that OSRM tends to slightly underestimate route distance, while Bing tends to overestimate distance relative to Google Maps. Interestingly, variation in the consistency of distance estimates can be observed between cities, with OSRM showing worse performance for the cities of Boston and New York, whereas Bing demonstrates worse performance for the cities of Boston and Atlanta. One of the reasons for discrepancies in distance estimates is that they were obtained for routes with a “shortest duration” goal, meaning that underlying differences between the engines regarding road segment speeds and delays can lead to differences in route selection and therefore distance.

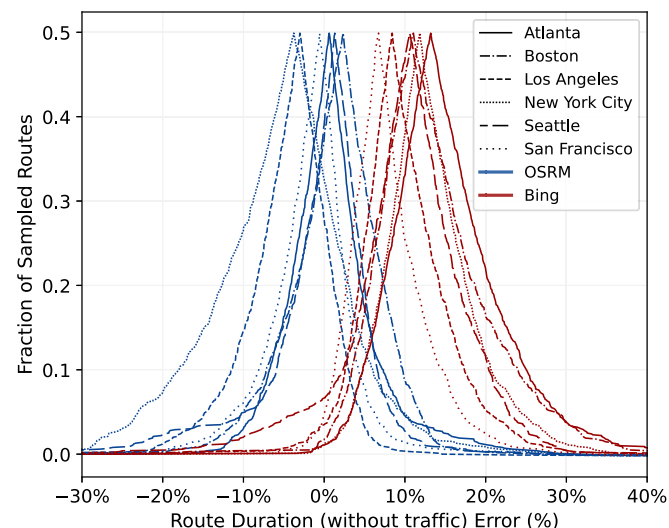
A comparison of duration estimations without traffic, illustrated in Fig. 4b, indicates greater variability between routing engines due to the increased complexity of estimating duration. A slight reduction in agreement can be observed for OSRM in most cities, with approximately 80% of routes remaining within 10% of the Google Maps duration estimate. New York is a notable exception, where only 70% of routes are within 10% error and the distribution is more heavily right skewed. Bing maps, however, show significantly more pessimistic estimates for route duration with only half of the routes falling within 10% of the Google Maps estimate. Discrepancies are in part due to inaccurate distance estimates but are also due to differences in how route duration is calculated between routing engines. Both the Bing and Google Maps routing engine provide duration estimates “without traffic” based on historical real-world data, meaning that traffic is still considered to some extent, particularly in cities that exhibit persistent high levels of traffic such as New York City and Los Angeles. In an effort to avoid historical traffic impacting the duration estimates, distance and duration estimates in Fig. 4 were obtained for 3:00 a.m. Sunday traffic. It should be noted that the “speed\_reduction” parameter in OSRM was set to 1.0 and the default speed table was modified to match speed limits typical of road type in the United States (speeds are based on road type if a speed limit is missing for a road segment). Google and Bing routing data were obtained with default API settings. The consideration of traffic data further increases the variability of route duration estimates as demonstrated in Fig. 5. Google and Bing routing data were obtained for 8:00 a.m. Tuesday traffic with default API settings, whereas TI-OSRM results were obtained from OSRM informed with congestion data from the speed-flow model. Baseline OSRM routing results were also included in Fig. 5 for comparison purposes.

Several observations can be made from Fig. 5: First, Bing Maps (depicted in red) tend to estimate significantly higher traffic congestion than the Google Maps routing engine. This is particularly apparent in Fig. 5a, where the median of the distribution can be



a) Folded CDF of Route distance error

Fig. 4 Routing API performance comparison for six major cities in the United States based on routing data without traffic from 1000 random routes in each city.



b) Folded CDF of route duration without traffic

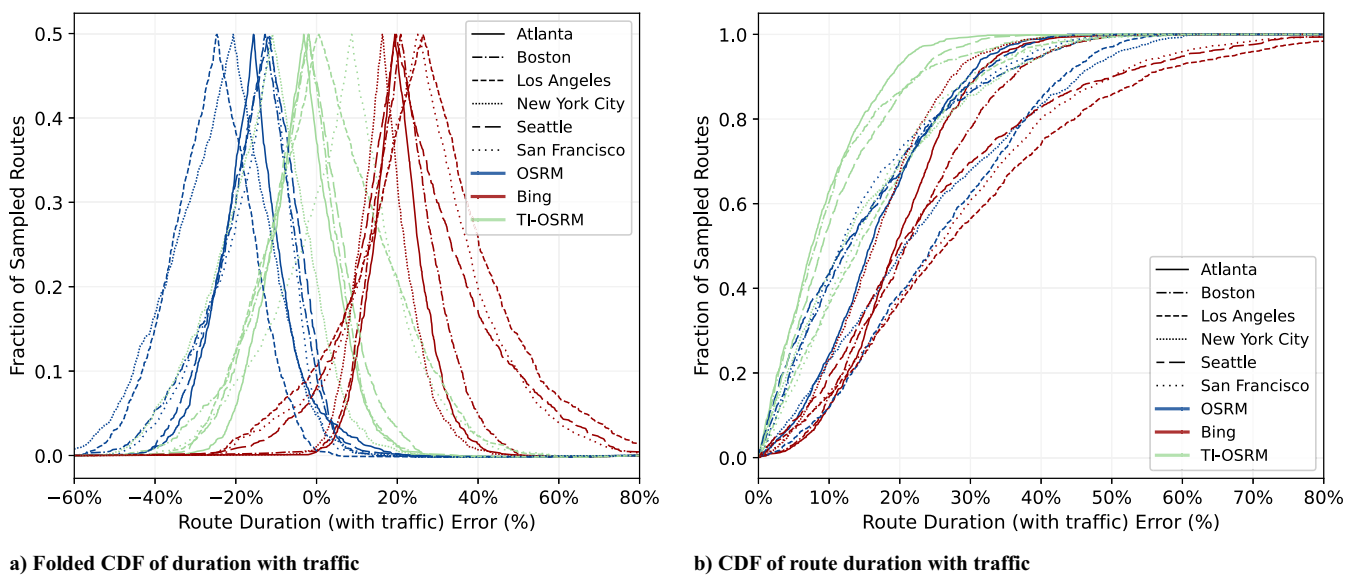


**Fig. 5** Routing API performance comparison for six major cities in the United States based on routing data obtained for 8:00 a.m. Tuesday traffic from 1000 random routes in each city.

observed to heavily favor the positive side of the error axis. This behavior is confirmed in Table 1, which shows that the mean error of the Bing Maps route duration ranges from 16 to 26%. This behavior demonstrates the variation in traffic estimation between the Google and Bing routing engines, and shows that the Bing routing engine again tends to provide a more pessimistic route duration relative to the Google Maps routing engine.

Second, and unsurprisingly, OSRM (depicted in blue) tends to significantly underpredict route duration data in cities where traffic is present due to the lack of consideration for traffic data. The mean error of the OSRM distribution can be improved by tuning parameters such as the “speed\_reduction” parameter in car.lua, but this approach significantly increases the standard deviation of the results and is not a suitable approach at the national level, where congestion levels vary significantly.

Lastly, and most significantly, the traffic-informed OSRM duration estimates (depicted in green) show substantial improvement relative to Bing Maps and the baseline OSRM estimates for all of the tested cities, with 93, 87, 67, 70, 86, and 71% of routes remaining within 20% of the Google Map routing engine duration estimates for Atlanta, Boston, Los Angeles, New York City, Seattle, and San Francisco, respectively. The improved performance can also be observed from Table 1, where the mean error and root-mean-squared error are improved without notable increase in standard deviation for routes in most cities. An improvement in the median of the TI-OSRM distribution relative to OSRM can also be observed in Fig. 5a. Error remains high for New York compared to the other cities in part due to the relatively large error for route duration without traffic. Error is also introduced by the uninformed constant nature of the assumed

directionality factor  $K$ , which leads to duration estimate errors for roads that experience the majority of traffic in the evening. It should be noted that accuracy improvements were also observed for all cities other than San Francisco relative to the baseline OSRM using a “speed\_reduction” factor of 0.8, which brings the mean of the baseline OSRM distributions more in line with Google Maps routing data (with traffic) but significantly increases the standard deviation of routing estimates in each city.

### B. Traffic Estimation Model Limitations

The implemented traffic estimation model has the advantage of relying only on public, national data sets; this flexibility, however, comes with several limitations.

First, congestion data lack directionality and time-of-day information, making it difficult to differentiate between morning and evening rush-hour congestion. The speed-flow model itself also lacks the ability to consider the impact of high-occupancy vehicle (HOV) lanes, lane or road closures, weather conditions, and the frequency of traffic incidents on roadway speeds.

Second, the speed-flow model primarily uses equations designed for uninterrupted flow, meaning that the model will underestimate congestion on signaled road segments with posted speed limits above 50 mph. Although OSRM imposes speed penalties on road segments with traffic lights and turns, other effects such as signal spacing, queue length, and pedestrian traffic (relevant for dense urban roads such as in New York City) are not considered. As a result, congestion on roads with posted speeds of 50 mph and below, particularly dense urban roads, is expected to be underestimated.

**Table 1 Comparison of OSRM,<sup>a</sup> TI-OSRM,<sup>b</sup> and Bing Maps<sup>c</sup> route duration error with traffic relative to the Google Maps<sup>d</sup> routing API**

City	Mean error			Root-mean-squared error			Standard deviation		
	OSRM	Bing	TI-OSRM	OSRM	Bing	TI-OSRM	OSRM	Bing	TI-OSRM
Atlanta	-15.8	19.9	-3.4	19.2	21.7	11.3	10.8	8.5	10.7
Boston	-14.7	21.5	-3.9	19.6	24.1	13.5	13.0	10.8	12.9
Los Angeles	-25.3	27.2	2.7	28.6	35.3	19.5	13.2	22.5	19.3
New York City	-22.8	16.7	-12.6	27.7	18.8	19.6	15.7	8.6	15.0
Seattle	-13.4	23.2	-2.8	18.4	30.1	13.5	12.5	19.3	13.2
San Francisco	-14.3	25.5	7.0	18.7	32.0	18.7	12.1	19.3	17.3

<sup>a</sup>Default car.lua parameter values modified as follows: speed\_reduction increased from 0.8 to 1.0; default speed table modified to match speed limits typical of road type in the United States.

<sup>b</sup>Traffic-informed OSRM (using the implemented traffic estimation model and a speed\_reduction value of 0.95).

<sup>c</sup>Routing data were obtained for 8:00 a.m. Tuesday traffic with default API settings.

Third, the speed-flow model also lacks specific consideration for oversaturated conditions (when the volume-to-capacity ratio exceeds unity) and is expected to underestimate congestion in these conditions, in part due to its inability to propagate congestion upstream when traffic blockages occur.

Lastly, error is introduced by the assumption that free flow speed is equal to posted speed limits and by the OSRM routing engine, which does not always find the fastest possible route for a given OD pair.

## V. Discrete Choice Demand Model

The discrete choice model forms the core of the demand estimation methodology by defining the probability of an individual choosing a UAM commuting service as a function of that individual's value of time as well as the time savings and costs relative to alternative modes of transportation. When modeling discrete mode choice, it is common to include a stochastic term that follows a certain distribution to account for unknown factors influencing the utility function [3]. For example, if an independent and identically distributed Gumbel distribution with a mode of zero and scale of one is used to model the stochastic term, the probability of an individual choosing a UAM commuting service between a given origin  $a$  and destination  $b$  can be defined as

$$P_u(a, b) = \frac{1}{1 + \exp(U_g - U_u)} \quad (11)$$

where  $U_g$  and  $U_u$  are the utilities associated with traveling by car and using a UAM service, respectively. This type of discrete choice model is known as a binary logit model. Given the novelty of UAM relative to existing modes of transportation and the associated uncertainty regarding public acceptance and ridership, selecting an appropriate shape for the stochastic term is difficult.

Several attempts at calibrating discrete choice models have been made using stated-preference surveys to estimate the stochastic term [20,21,49]; however, results from the stated preference surveys are not broadly consistent, likely as a result of differing survey design approaches and the continuing evolution of public awareness of UAM between the time periods in which the surveys were conducted. Hill and Garrow [19] found a negative shift in perception toward UAM in surveys conducted from 2018 to 2021. Specifically, 51% of 2021 survey participants were cautiously enthusiastic or had mixed sentiments toward UAM compared to 34% in 2018, and 38% were enthusiastic in 2021 compared to 57% in 2018. Fu et al. [20] and Al Haddad et al. [21] presented survey participants with hypothetical transportation scenarios to better understand likely adoption of a UAM service. Fu et al. found total travel time to be the most influential parameter to service adoption and found that less educated individuals and older individuals are less likely to use a UAM service but found no adoption difference between genders and no clear trend between income and adoption rate. Adoption rate was also found to vary significantly based on trip purpose (such as commuting, business, shopping, social activities). Al Haddad, on the other hand, found highly educated respondents less likely to be early adopters of UAM and found female respondents to be generally less likely to adopt UAM than their male counterparts. Trip cost and duration were found to be important characteristics to UAM adoption, but mode safety was found to be the most influential parameter to UAM adoption.

Given the steepness of the curve described by Eq. (11) and to keep the model general and applicable to any region, we chose to remove the stochastic term entirely and to simplify Eq. (11) into a deterministic model defined by Eq. (12). With this simplification, an individual is considered a potential UAM customer if the UAM service provides a higher utility than car-based transportation.

$$P_u(a, b) = \begin{cases} 1, & \text{if } U_u > U_g \\ 0, & \text{otherwise} \end{cases} \quad (12)$$

The utility of each mode of transportation is based on the cost of the transportation mode to the individual and is made up of costs directly

associated with the mode of transportation ( $c_m$ ), time-based costs that are a function of the value of time ( $V$ ) of the individual, and the trip duration ( $t_{m,a \rightarrow b}$ ). This general formulation is given in Eq. (13). The negative sign is present because both terms represent costs or disutilities to the individual.

$$U_m = -(Vt_{m,a \rightarrow b} + c_m) \quad (13)$$

Past research in the transportation literature [50] has found that it is possible to relate the value of time savings to hourly income, depending on the purpose of the trip. For a business trip, the value of time has been shown to be 0.8–1.2 of the hourly household income of the individual, whereas the factor ranges between 0.6 and 0.9 for a personal trip [50]. In this work, a factor of one is used to relate an individual's value of time savings to their hourly income given that commuting to work can be considered a business trip. Assuming an individual's annual income of  $x$  is earned over 52 work weeks, with 40 work hours per week, his or her value of time (in units of \$ per minute) can be defined as

$$V = \frac{x}{124,800} \quad (14)$$

The utility functions specific to a UAM and car-based transportation service are provided in Eqs. (15a) and (15b), respectively. Whereas trip duration for a purely ground-based transportation is simply denoted by  $t_{g,O \rightarrow D}$ , the UAM commuting service is modeled on the assumption that ground transportation will be necessary to bring an individual from the point of origin to the nearest vertiport ( $t_{g,O \rightarrow V_O}$ ) and to the final destination from the destination vertiport ( $t_{s,V_D \rightarrow D}$ ); hence, the total trip duration for a UAM commuting service is the sum of  $t_{g,O \rightarrow V_O}$ ,  $t_{e,V_O \rightarrow V_D}$ , and  $t_{s,V_D \rightarrow D}$ .

$$U_u = -(V(t_{g,O \rightarrow V_O} + t_{e,V_O \rightarrow V_D} + t_{s,V_D \rightarrow D}) + c_e + c_s + \tilde{c}_g d_{g,O \rightarrow V_O}) \quad (15a)$$

$$U_g = -(Vt_{g,O \rightarrow D} + \tilde{c}_g d_{g,O \rightarrow D}) \quad (15b)$$

Costs for a purely ground-based transportation mode include the car operational and maintenance costs,  $\tilde{c}_g$ . Due to the multimodal nature of a UAM transportation service, however, both a ticket price for the flight portion of the trip and ground-based operational costs need to be considered.

UAM ticket costs, given by Eq. (16a), are assumed to be the only direct cost of a UAM service to potential customers, and are composed of a fixed and variable component, where the variable component is a function of the distance flown by the UAM vehicle,  $d_{e,V_O \rightarrow V_D}$ . Pricing for the mode of transportation of the last leg, given in Eq. (16b), is assumed to be for a secondary mode of transportation, such as a taxi, ride hailing service, or electric scooter.

$$c_e = \check{c}_e + \tilde{c}_e d_{e,V_O \rightarrow V_D} \quad (16a)$$

$$c_s = \check{c}_s + \tilde{c}_s d_{s,V_D \rightarrow D} \quad (16b)$$

Finally, potential commuter demand for a UAM commuting service between an OD pair is given by Eq. (17). The total potential demand for a particular area, i.e., the number of commuters along every OD pair for whom the UAM commuting service provides an increase in utility, is given by Eq. (17b). It should be noted that since the speed and cost associated with each considered mode of transportation can be customized, the presented model can easily be generalized to consider alternative or additional modes of transportation for each trip leg.

$$\Pi_u(a, b) = N_{a \rightarrow b} P_u(a, b) \quad (17a)$$

$$\Pi_u = \sum_{(a,b)}^{S_{O \rightarrow D}} N_{a \rightarrow b} P_u(a, b) \quad (17b)$$

Calculating demand using Eq. (17) is not straightforward, however, because the annual income of commuters between an OD pair is not uniform, meaning that the value of time and therefore the utility of each mode of transportation are not necessarily uniform for all commuters corresponding to an OD pair. Since we are using a deterministic mode choice model, we can calculate the annual income required for the utility of a UAM service to be equal to or greater than the utility of ground-transportation ( $U_u \geq U_g$ ) rather than calculating utilities for every income level.

By introducing the notation  $\check{x}$  to represent the minimum required income for  $U_u \geq U_g$ , sometimes referred to as the break-even income, we can rearrange Eq. (14) into Eq. (18).

$$\check{x} = 124,800V \quad \text{such that } U_u \geq U_g \quad (18)$$

Combining Eqs. (15a) and (15b) and enforcing  $U_u \geq U_g$ , we can isolate and replace  $V$  to obtain Eq. (19):

$$\check{x} = 124,800 \left( \frac{c_e + c_s + \tilde{c}_g d_{g,O \rightarrow V_O} - \tilde{c}_g d_{g,O \rightarrow D}}{t_{g,O \rightarrow D} - t_{g,O \rightarrow V_O} - t_{e,V_O \rightarrow V_D} - t_{s,V_D \rightarrow D}} \right) \quad (19)$$

where the numerator of Eq. (19) represents effective ticket cost and the denominator represents time savings. Lastly, we can rewrite Eq. (17) as Eq. (20), where  $N_{\check{x},a \rightarrow b}$  is the number of individuals with a daily commute from  $a$  to  $b$  whose annual income is at least  $\check{x}$ .

$$\Pi_u(a, b) = N_{\check{x},a \rightarrow b} \quad (20a)$$

$$\Pi_u = \sum_{(a,b)}^{S_{O \rightarrow D}} N_{\check{x},a \rightarrow b} \quad (20b)$$

Formulating the demand model in this manner greatly simplifies determination of demand since the distribution of income is known for every OD pair. The scalability and speed of the developed demand methodology makes it suitable for optimization, e.g., as part of demand-based vertiport placement or vehicle-scheduling optimization.

#### A. Demand Model Limitations and Assumptions

Implicit to the deterministic formulation of the mode choice model is the assumption that individuals behave rationally and will select the mode of transportation that maximizes their utility. A number of factors likely to impact demand are also not considered within the utility functions, such as willingness to fly on UAM vehicles, ownership of a car, or availability of alternative modes of transportation to reach nearby vertiports, and ability to complete the last leg of the journey (between the workplace and the nearest vertiport) [17,21]. Several important operational constraints are also not considered by the demand model, namely, the operational capacity of vertiports, weather impacts, and noise constraints.

Ground-transportation costs are based on car operational and maintenance costs rather than ride hailing or public transportation costs under the assumption that individuals have access to a car and that car-based transportation is the most competitive alternative mode of transportation relative to a UAM service due to the lower cost, lower trip duration, and lack of mode changes involved with driving a personal vehicle. This assumption is expected to lead to an overestimation of potential demand for cities with well-developed transportation networks, specifically for commuting routes that already have efficient, direct connections through a rapid transit system. As a result, this assumption may not be valid in regions outside of North America, where bus and rail options are often more convenient than driving. Within the United States, the omission of public transit as a mode choice is expected to have a negligible impact on demand, with the exception of certain major cities such as New York City and Washington, DC, which have more established transit systems. The mode choice formulation, however, can easily be adapted to include public and on-demand ground transportation services. Car operational costs are assumed to be \$0.126/km (20.28 ¢ per mile) and are based on the

**Table 2 Demand model parameters**

Parameter	Description	Value
$t_{\text{delay}}$	Total service delay time	0–30 min
$v_e$	UAM vehicle cruise speed	300 km/h
$\check{c}_e$	Fixed UAM ticket price	5.00 \$
$\tilde{c}_e$	Variable UAM ticket price	0.25–5.00 \$/km
$\tilde{c}_g$	Car operational cost	0.126 \$/km

2021 weighted average car operational (fuel + maintenance) cost provided by the American Automobile Association [51].

A representative cruise speed of 300 km/h is assumed for UAM operations based on the Joby S4 (322 km/h) and Archer Midnight (241 km/h) vehicles [52,53], given that they have received electric vertical takeoff and landing (eVTOL) airworthiness criteria from the Federal Aviation Administration (FAA) [54,55]. A range of cruise speeds is not considered because an increase in cruise speed is expected to have a similar (but muted) impact on potential demand as a decrease in ticket price per kilometer.

Ticket pricing is based on estimates from Uber Elevate and Booz Allen Hamilton [4,26], who predicted pricing to be 1.85–\$6.84/km in the near-term and \$0.29–1.55/km in the far-term. An additional fixed ticket cost of \$5.00 is added to avoid the formation of unrealistically short UAM routes with near-zero ticket prices.

Lastly, a total service delay time between 0 and 30 min is assumed to account for the time required for passenger boarding and deplaning, and for differences in forward speed during takeoff, cruise-climb, descent, and landing relative to the cruise speed.

A summary of the variables with assumed values relevant to the discrete choice demand model is provided in Table 2.

#### B. Simplifications for Nationwide Modeling

All components of the demand modeling methodology perform well at a nationwide scale except for vertiport location identification, due to the limited scalability of vertiport placement optimization algorithms. As a result, to enable nationwide demand modeling, we assume that vertiports exist at all origin and destination locations, meaning that  $V_O = O$  and  $V_D = D$ . The time associated with travel to and from a finite set of vertiport locations is instead absorbed by the total service delay time  $t_{\text{delay}}$ .

With this assumption, the utility function for a UAM vehicle, given by Eq. (15a), can be simplified to

$$\tilde{U}_u = -(V t_{e,O \rightarrow D} + \check{c}_e + \tilde{c}_e d_{e,O \rightarrow D}) \quad (21)$$

Unless specified otherwise, all references to approximate demand estimation, and use of  $\tilde{U}_u$  refers to Eq. (21). Alternatively, we could assume that vertiports coincide with existing ground infrastructure, such as private and public airports and helipads. This assumption, however, significantly reduces demand estimates for regions where facilities do not currently exist near city centers. Given that the capacity of such facilities is not being modeled and the potential to build new vertiport infrastructure, we chose not to constrain vertiport locations to existing private and public airports and helipads.

## VI. Results and Discussion

Nationwide demand estimates were obtained using the simplified methodology described in Sec. V and using the parameters described in Table 2. A total service delay time of 10 min and a ticket price of \$1.85/km (with a base ticket price of \$5) are used for all results with the exception of sensitivity studies specific to those parameters. Note that demand estimates obtained with this methodology should not be used directly without additional considerations for vertiport placement, vertiport operational capacity, weather constraints, and community noise constraints. Results obtained without these additional constraints are still valuable, however, to identify cities of interest for UAM operations, estimating long-term demand potential, and

analyzing sensitivity of demand to parameters such as ticket price and total trip delay time.

A geographic distribution of demand density (customers per square kilometer) in counties across the United States is first presented in Fig. 6. Unsurprisingly, demand is focused around urban centers due to the larger population density, high traffic congestion, and the larger number of high-income individuals, whose value of time and willingness to use a UAM service are assumed to be greater. Demand in Fig. 6 is normalized by county area (referred to as demand density) to avoid demand being biased toward larger counties.

Counties near the cities of New York, San Francisco, Los Angeles, Boston, Chicago, and Washington, DC, stand out as having demand densities above 10 customers per square kilometer for the baseline

UAM commuting mission (10-min total service delay time, \$5.00 base ticket price, \$1.85/km variable ticket price). Other major metropolitan areas such as Atlanta, Seattle, Philadelphia, Houston, and Denver demonstrate demand densities between 5 and 10 customers per square kilometer. It should be noted that a logarithmic scale is used in Fig. 6 and throughout this section to better illustrate variations in demand across the country.

To better illustrate demand distribution for near-term UAM operations, the maximum possible total ticket price that provides a demand density of 10 customers per square kilometer was calculated and is provided in Fig. 7. Unsurprisingly, the majority of cities can support a demand density of 10 with a \$10 total ticket price (no ticket price per kilometer is enforced). The cities of New York, San Francisco,



**Fig. 6** Geographic distribution of demand density in the United States.

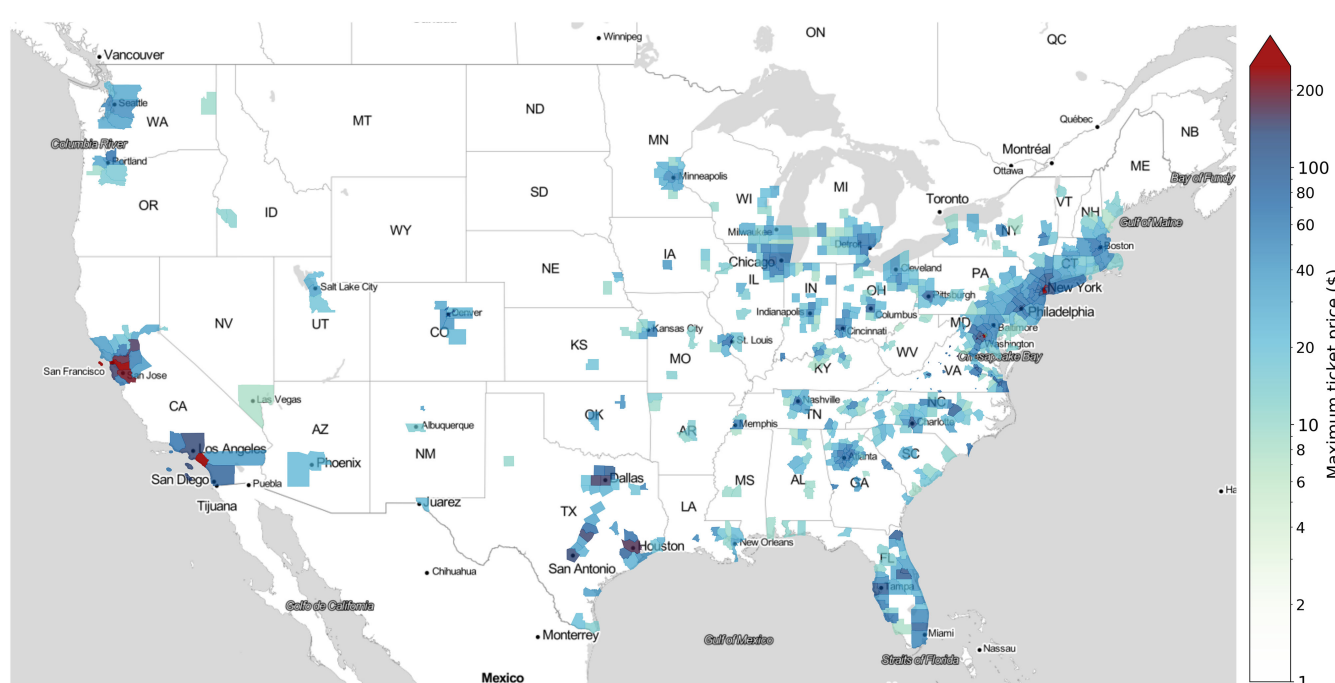


**Fig. 7** Geographic distribution of maximum ticket price in the United States to meet a minimum demand density of 10 customers per square kilometer.

Washington, DC, Dallas, and Houston are most notable in this case, providing a demand density of 10 with a ticket price near or above \$100.

Results in Fig. 7 become more interesting, however, when considered alongside Fig. 8, which illustrates the maximum variable ticket price (\$ per kilometer) if the base ticket price is fixed to \$5. Together, the results show that high demand exists for longer range missions (100–200 km), which could be a strong market for UAM if operational costs allowed a sufficiently low \$ per kilometer pricing (e.g., if UAM vehicles are unmanned and charging and maintenance costs are low).

In the near-term, when operational costs are likely to be higher, the cities of New York and San Francisco seem best suited from a demand standpoint, given that a demand density of 10 customers per square kilometer is retained with ticket prices above \$2.50/km, with higher pricing likely possible in subdivisions of the highlighted counties. A close resemblance can be observed between Figs. 6 and 8 given that

the demand density in Fig. 8 is equivalent to Fig. 6 when the ticket price is \$5 + \$1.85/km.

Lastly, sensitivity results that demonstrate the impact of total service delay time and ticket price per kilometer are presented in Figs. 9a and 9b, respectively. Figure 9a suggests that a logarithmic relationship exists between potential demand and total service delay time, highlighting the importance of time savings in the implemented demand model. For example, New York City shows a demand of 600,000 with a total delay of 5 min but only 40,000 with a delay of 15 min. This result is not surprising due to the assumption that vertiports exist near every origin and destination location, meaning that demand exists for all commuters with nontrivial commutes and moderate incomes. As the delay time increases, however, demand is limited to commuters who experience longer and more congestion or less direct commutes, and have a higher value of time. Seattle is an interesting exception, where a much lower rate of decrease in demand can be observed for total delay times greater than 15 min. This result

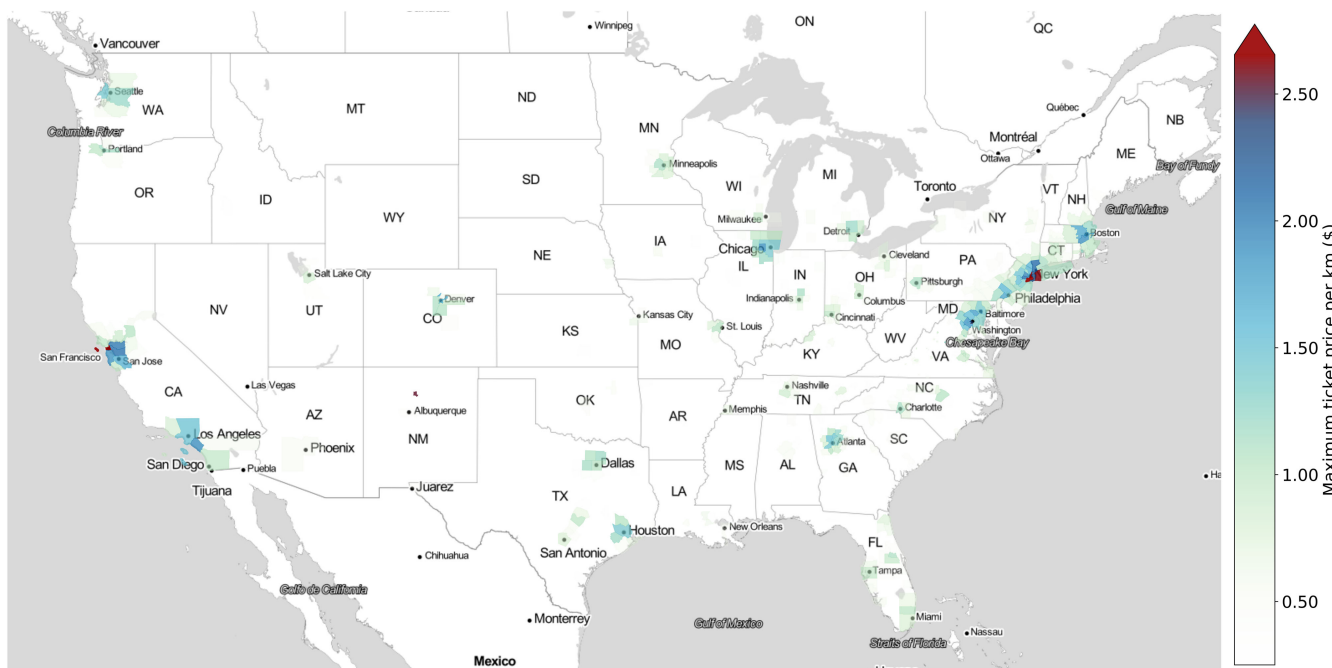
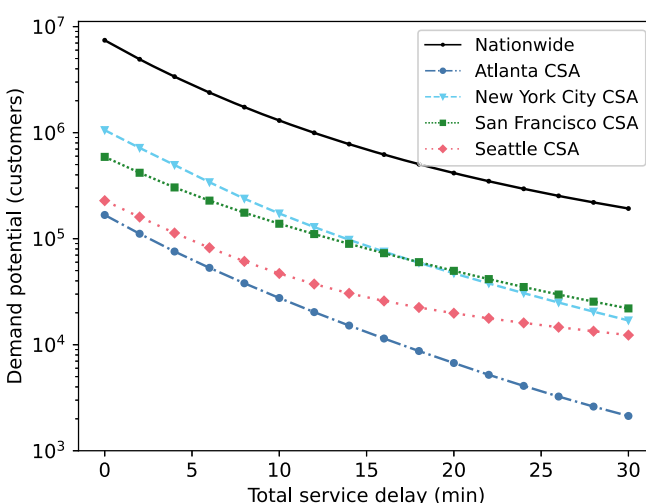
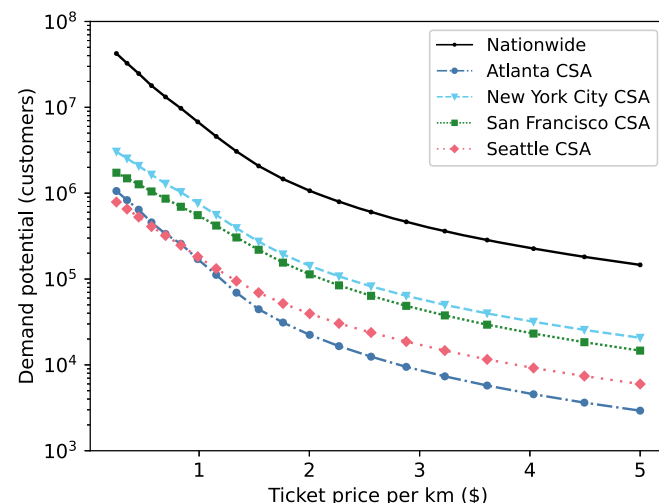


**Fig. 8** Geographic distribution of maximum ticket price per kilometer in the United States to meet a minimum demand density of 10 customers per square kilometer.



a) Sensitivity of demand to time delays



b) Sensitivity of demand to changes in ticket price per km

**Fig. 9** Sensitivity of demand to time delay and ticket price per kilometer.

is likely due, in part, to the lack of bridges and tunnels across Puget Sound in Seattle, thereby requiring residents on the west side of the Sound to use a ferry service or to make a significant detour in order to reach Seattle. San Francisco exhibits a similar but weaker transition, likely also due to the topology of the area, which requires detours to reach bridges or to avoid mountainous areas (note that a direct flight was assumed for all OD pairs, regardless of topography).

Figure 9b, on the other hand, suggests that the sensitivity of demand to ticket price per kilometer has three distinct regions: the first region, with a ticket price between \$0.25/km and \$1.50/km, shows a steep logarithmic relationship denoting a rapid decline in demand as longer missions become cost inefficient and low value shorter missions become untenable. The second region, between \$1.50/km and \$3.00/km, is a transitory region that exhibits a gradually decreasing sensitivity to ticket price. The last region, between \$3.00/km and \$5.00/km, becomes logarithmic again, although at a shallower slope due in part to the smaller range of the remaining commutes that exhibit demand for a UAM service. Atlanta exhibits a greater initial dependency on ticket price per kilometer than the other cities due to the sprawling nature of the Atlanta region, where the majority of the population lives in suburbs far from the city. It should be noted that results provided in Fig. 9 specifically refer to the Atlanta–Athens–Clarke County–Sandy Springs, GA Combined Statistical Area (CSA); New York–Newark, NY–NJ–CT–PA CSA; San Jose–San Francisco–Oakland, CA CSA; and Seattle–Tacoma, WA CSA.

Figure 10, which shows the sensitivity of demand to total delay time and ticket price per kilometer on the same plot, demonstrates the coupling between these parameters at the national and regional scale more clearly. We can see that demand becomes increasingly sensitive to changes in ticket price, particularly for low ticket prices, as the total time delay increases, shown by an increase in slope in Figs. 10a and 10b. This behavior occurs because demand becomes composed of longer and longer trips as the total delay time increases, resulting in a greater decrease in demand when ticket price per kilometer is increased for trips with a high total delay time. Alternatively, we can also say that routes with a higher ticket price per kilometer are primarily composed of shorter trips and are therefore significantly more sensitive to increases in total delay time.

Overall these results demonstrate that significant demand for a commuting UAM mission exists but that it scales in a logarithmic fashion with total service delay time and with ticket price per kilometer, meaning that a widespread UAM commuting service would require numerous vertiports and minimal delays associated with routing and scheduling, and ticket prices would need to rival ground-taxi services. These results also show, however, that reasonable demand is retained in several cities even when the total service delay time and ticket price per kilometer are independently increased

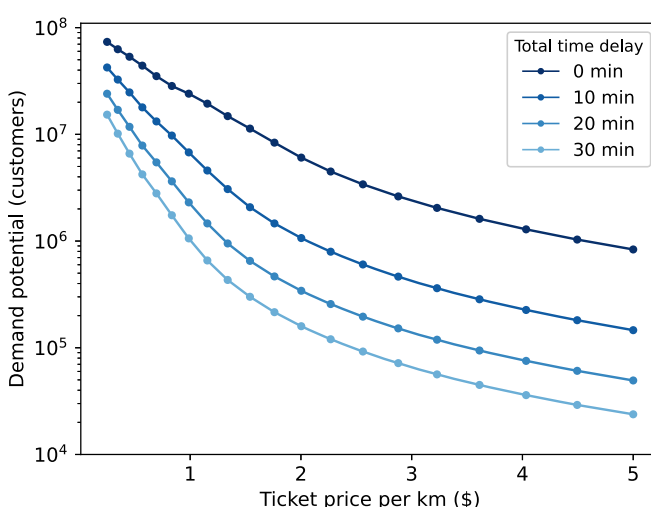
to 30 min and \$5/km, respectively, particularly the cities of New York, San Francisco, and Seattle. Lastly, the compounding effect of changes in total delay time and ticket price per kilometer has demonstrated that demand is significantly reduced if both long delays and high ticket price per kilometer values are present due to the elimination of two primary customer pools: 1) customers with long commutes for whom an increase in ticket price per kilometer results in an unaffordable ticket, and 2) customers with shorter commutes for whom an increased delay time eliminates any time savings. In the case that neither the total time delay nor ticket price per kilometer can be kept small, which may be the case for near-term UAM operations, commuting missions in which the flight path distance is significantly shorter than the drive distance, such as flights over Puget sound in Seattle, would provide the most benefit to the customer. Alternatively, routes currently served only by ferry, airplane, or helicopter, such as between Victoria and Vancouver in Canada, are ideal.

#### A. Comparison to Previous Studies

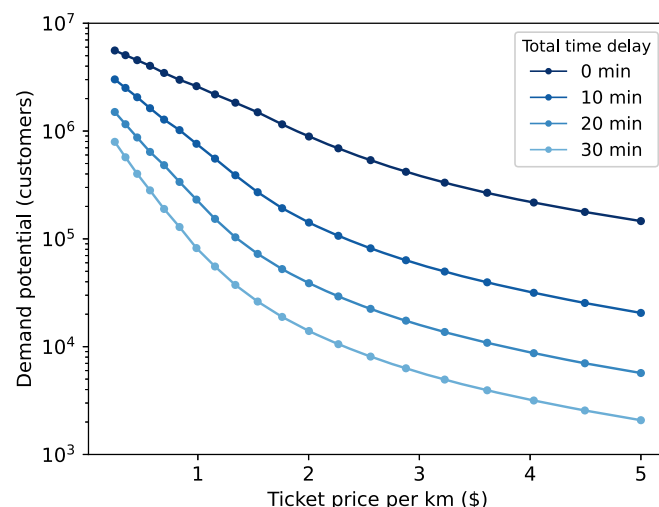
A number of studies and reports have been published that rank and compare demand in cities in the United States. Although demand estimates and rankings between these studies are not expected to match given significant differences in methodology, assumptions, and types of UAM services being modeled, comparing results at a high level with these differences is worthwhile. Estimates of demand for a larger set of CSAs are provided in Fig. 11 as a basis for comparison and discussion with some of these studies.

The study by Haan et al. [12], in which a calibrated multinomial logit model was applied to cellphone location data and census income data to compare commuter demand across 40 combined statistical areas, is the most similar in scope to our work given that it also aims to estimate demand for a commuter UAM mission. Nonetheless, it differs in several important respects: 1) vertiport locations are assumed to coincide with existing private and public airports and helipads rather than existing at all origins and destinations, 2) cellphone data are used to determine commuter flow in each city rather than the LODES database, and 3) a calibrated multinomial logit mode choice model is used rather than a discrete choice model. Nevertheless, results show reasonable agreement for the majority of CSAs compared in Fig. 11.

San Francisco is a notable exception, where our estimated demand is significantly higher. This difference is primarily a result of the assumption made by Hann et al. that vertiport locations exist only at locations designated as private and public airports and helipads. As noted by the authors, no such infrastructure exists near the central business district in San Francisco, significantly reducing time savings and thereby demand for commuters who live or work in the area. The San Francisco CSA also has the lowest density of existing “vertiport”



a) National demand sensitivity



b) Demand sensitivity in New York City CSA

Fig. 10 Sensitivity of demand to changes in both time delay and ticket price per kilometer.

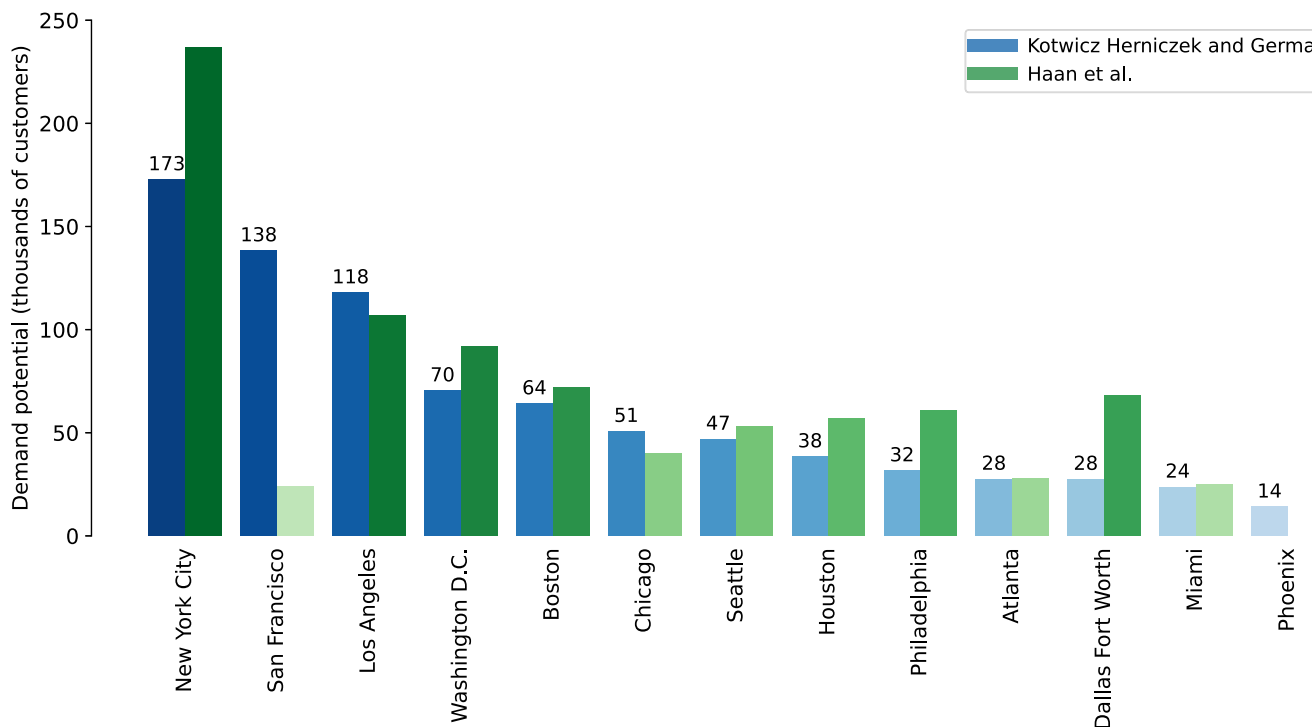


Fig. 11 Commuter demand estimates for some of the most populous CSAs in the United States (total delay time of 10 min and a ticket price of \$5 + \$1.85/km) compared to demand estimates from Haan et al. [12].

infrastructure relative to the 40 cities analyzed, effectively increasing the total delay time for a significant portion of routes in the area, thereby significantly reducing demand. Additionally, traffic congestion in San Francisco was overestimated by our speed-flow congestion model, increasing time savings for routes in the area and consequently increasing UAM demand in San Francisco.

Differences in demand estimates for Philadelphia are likely due in part to the fact that Philadelphia has the highest density of existing infrastructure out of the cities presented in Fig. 11, effectively decreasing the total delay time associated with routes in the area and increasing demand. Underprediction of demand for New York City can be attributed, in part, to underestimation of congestion by the speed-flow congestion model. Lastly, discrepancies in the demand estimates for the Dallas–Fort Worth CSA may be due to the small sample size of the cellphone data used by Haan et al. for the region. Any inconsistencies within the data would significantly impact the demand estimate for the region due to the scaling necessary to match the number of trips to census data. The remaining reports that compare demand in cities in the United States are less similar in scope to our work and consequently provide demand estimates that differ by orders of magnitude. The order of city rankings, however, remains relatively consistent with our work due to the dependence of demand on population density, income distribution, and time savings.

Booz Allen Hamilton [4] published a market study for near-term UAM operations with demand estimates based on a modified four-step modeling approach that relied on several data sets for trip generation, including the ACS, National Travel Household Survey (NTHS), and Bureau of Transportation Statistics (BTS) T-100 (Airline Passenger) Market data. A gravity model was used to distribute trips between census tracts, and a calibrated multinomial logit model was used for mode choice. Demand estimates for an unconstrained scenario (where vertiports exist in each census tract and demand is not constrained by customer willingness to pay) were found to be 1,421,000 in New York City and 422,000 in Phoenix, with Los Angeles, Dallas, Miami, Houston, San Francisco, and Washington, DC, in between. Introduction of constraints on willingness to pay and limiting infrastructure to existing private and public airports and heliports reduced demand estimates to similar levels as those presented in Fig. 11. For example, estimates for demand in NYC and Washington, DC, are 127,000 and 59,000, respectively. It should

be noted, however, that demand estimates in this report included demand for discretionary trips (shopping, restaurants) and airport-shuttle trips in addition to commuting demand. The report also found that demand dropped another order of magnitude when infrastructure capacity constraints were introduced, highlighting the importance of vertiport capacity as a constraint.

Lastly, KPMG [6] released a report that estimated demand based on city Gross Domestic Product (GDP), population, growth, wealth concentration, intracity travel times, congestion, alternative modes of transportation, and limousine service utilization. The report projected demand for intracity airport shuttles in 2030 to be 700,000 and 100,000 customers in New York City and Phoenix, respectively. New York City was ranked highest, followed by Los Angeles, Chicago, Dallas, Houston, San Francisco, Washington, DC, and Phoenix. Direct comparison is difficult due to the lack of published methodology in KPMG's report; however, we can postulate based on their ranking that their methodology was perhaps more dependent on population size and GDP than the demand model implemented in this work.

## VII. Conclusions

A scalable, discrete mode-choice demand model for UAM capable of demand estimation at the national level was developed that enables fast demand estimation based on the relative utility of available travel modes. The demand model uses LODES flow data, ACS economic data, and OSRM to identify the utility of a UAM commuter service relative to other modes of transportation. The demand model is supported by a speed-flow model, which fuses HPMS and OSM data to provide traffic-adjusted road segment speeds to OSRM. The implemented traffic estimation model significantly improved route duration estimates in congested areas, decreasing the average mean square error of trip duration relative to Google Maps from 22 to 16% (averaged over the cities considered in the analysis). Both the traffic estimation and demand estimation model were built around publicly available, national data sets in an effort to increase reproducibility and utility of the models.

The demand model was applied at a national scale and identified counties within the cities of New York, San Francisco, Los Angeles, and Washington, DC, as having the highest demand density and

highest overall demand for a UAM commuting service. The results suggest that counties in these cities can support ticket prices of \$200 per trip and maintain a demand density of 10 customers per square kilometer but that these same counties can only support pricing of 2.5 \$ per kilometer, highlighting that significant demand exists for longer UAM trips.

A sensitivity study of demand to changes in ticket prices and total trip delay time was performed and showed that a logarithmic relationship exists between potential demand and total service delay time, whereas demand is more sensitive to change in ticket price per kilometer at low ticket-price-per-kilometer values. Seattle was a notable exception, where demand was relatively insensitive to increases in total delay time for delays larger than 15 min. Results also showed that demand becomes increasingly sensitive to changes in ticket price (particularly for low ticket prices) as the total time delay increases. This is because demand increasingly consists of longer and longer trips as the total delay time increases, resulting in a greater decrease in demand when ticket price per kilometer is increased for those trips. Likewise, routes with a higher ticket price per kilometer are primarily composed of shorter trips and are therefore significantly more sensitive to increases in total delay time.

UAM demand estimates were also compared to several published studies. Reasonable agreement and similar city rankings were found relative to other studies, even with significant differences in methodology, highlighting the large impact of population density and income distribution on demand, which were consistent across each study. San Francisco was a notable exception, where limiting vertiport locations to existing public private and public airports led other studies to estimate significantly lower demand for the region, demonstrating that limiting UAM operations to existing airport and helipad infrastructure significantly limits potential demand in some regions.

Several important limitations exist in the presented models. Namely, vertiport operational capacity, weather constraints, and community noise constraints are not considered in the demand model. Additionally, vertiport infrastructure is assumed to exist at each OD pair in the simplified nationwide version of the demand model. Consequently, demand estimates from this method should not be used directly without additional considerations, particularly consideration for vertiport placement and vertiport operational capacity. Nevertheless, results obtained with the implemented demand model provide meaningful insight into cities of interest for UAM operations, the long-term demand potential of a UAM commuting service, and the sensitivity of demand to parameters such as ticket price and total trip delay time.

## Acknowledgment

This work was partially supported by NASA through cooperative agreement 80NSSC21M0113: Innovative Manufacturing, Operation, and Certification of Advanced Structures for Civil Vertical Lift Vehicles (IMOCAS).

## References

- [1] Profillidis, V. A., and Botzoris, G. N., *Modeling of Transport Demand: Analyzing, Calculating, and Forecasting Transport Demand*, Elsevier, New York, 2018, Chap. 3, <https://trid.trb.org/view/1584028>.
- [2] McNally, M. G., "The Four-Step Model," *Handbook of Transport Modelling*, edited by D. A. Hensher, and K. J. Button, Vol. 1, Emerald Group Publishing Limited, Bingley, England, U.K., 2007, pp. 35–53. <https://doi.org/10.1108/9780857245670-003>
- [3] Garrow, L. A., *Discrete Choice Modelling and Air Travel Demand: Theory and Applications*, Ashgate, Farnham, England, U.K., 2010, Chaps. 1 and 3.
- [4] Goyal, R., Reiche, C., Fernando, C., Serrao, J., Kimmel, S., Cohen, A., and Shaheen, S., "Urban Air Mobility (UAM) Market Study," NASA HQ-E-DAA-TN65181, Nov. 2018, <https://ntrs.nasa.gov/citations/20190001472>.
- [5] NEXA Advisors, "Urban Air Mobility—Economics and Global Markets," NEXA Advisors TR, McLean, VA, 2018.
- [6] Mayor, T., and Anderson, J., "Getting Mobility Off the Ground," KPMG TR, 2019.
- [7] Syed, N., Rye, M., Ade, M., Trani, A., Hinze, N., Swingle, H., Smith, J. C., Dollyhigh, S., and Marien, T., "Preliminary Considerations for ODM Air Traffic Management Based on Analysis of Commuter Passenger Demand and Travel Patterns for the Silicon Valley Region of California," *17th AIAA Aviation Technology, Integration, and Operations Conference*, AIAA Paper 2017-3082, 2017. <https://doi.org/10.2514/6.2017-3082>
- [8] Ploetner, K. O., Al Haddad, C., Antoniou, C., Frank, F., Fu, M., Kabel, S., Llorca, C., Moeckel, R., Moreno, A. T., Pukhova, A., Rothfeld, R., Shamiyah, M., Straubinger, A., Wagner, H., and Zhang, Q., "Long-Term Application Potential of Urban Air Mobility Complementing Public Transport: An Upper Bavaria Example," *CEAS Aeronautical Journal*, Vol. 11, No. 4, 2020, pp. 991–1007. <https://doi.org/10.1007/s13272-020-00468-5>
- [9] Rimjha, M., and Trani, A., "Urban Air Mobility: Factors Affecting Vertiport Capacity," *2021 Integrated Communications Navigation and Surveillance Conference*, IEEE, New York, 2021, pp. 1–14. <https://doi.org/10.1109/ICNS2807.2021.9441631>
- [10] Wu, Z., and Zhang, Y., "Integrated Network Design and Demand Forecast for On-Demand Urban Air Mobility," *Engineering*, Vol. 7, No. 4, 2021, pp. 473–487, <https://www.sciencedirect.com/science/article/pii/S2095809921000837>. <https://doi.org/10.1016/j.eng.2020.11.007>
- [11] Justin, C. Y., Payan, A. P., and Mavris, D., "Demand Modeling and Operations Optimization for Advanced Regional Air Mobility," *AIAA Aviation 2021 Forum*, AIAA Paper 2021-3179, 2021. <https://doi.org/10.2514/6.2021-3179>
- [12] Haan, J., Garrow, L. A., Marzuoli, A., Roy, S., and Bierlaire, M., "Are Commuter Air Taxis Coming to Your City? A Ranking of 40 Cities in the United States," *Transportation Research Part C: Emerging Technologies*, Vol. 132, Nov. 2021, Paper 103392, <https://www.sciencedirect.com/science/article/pii/S0968090X21003892>. <https://doi.org/10.1016/j.trc.2021.103392>
- [13] Straubinger, A., Verhoef, E. T., and de Groot, H. L. F., "Will Urban Air Mobility Fly? The Efficiency and Distributional Impacts of UAM in Different Urban Spatial Structures," *Transportation Research Part C: Emerging Technologies*, Vol. 127, June 2021, Paper 103124, <https://www.sciencedirect.com/science/article/pii/S0968090X21001431>. <https://doi.org/10.1016/j.trc.2021.103124>
- [14] Kotwicz Heniczek, M. T., Garbo, A., Lau, M., German, B., and Garrow, L., "Exploration of Near-Term Urban Air Mobility Operations with Retrofitted Electric General Aviation Aircraft," *AIAA Aviation 2019 Forum*, AIAA Paper 2019-2872, 2019. <https://doi.org/10.2514/6.2019-2872>
- [15] Bulusu, V., Onat, E. B., Sengupta, R., Yedavalli, P., and Macfarlane, J., "A Traffic Demand Analysis Method for Urban Air Mobility," *IEEE Transactions on Intelligent Transportation Systems*, Vol. 22, No. 9, 2021, pp. 6039–6047. <https://doi.org/10.1109/TITS.2021.3052229>
- [16] Alvarez, L. E., Jones, J. C., Bryan, A., and Weinert, A. J., "Demand and Capacity Modeling for Advanced Air Mobility," *AIAA Aviation 2021 Forum*, AIAA Paper 2021-2381, 2021. <https://doi.org/10.2514/6.2021-2381>
- [17] Garrow, L. A., German, B., Mokhtarian, P., Daskilewicz, M., Douthat, T. H., and Binder, R., "If You Fly It, Will Commuters Come? A Survey to Model Demand for eVTOL Urban Air Trips," *2018 Aviation Technology, Integration, and Operations Conference*, AIAA Paper 2018-2882, 2018. <https://doi.org/10.2514/6.2018-2882>
- [18] Garrow, L. A., Mokhtarian, P., German, B., and Boddupalli, S.-S., "Commuting in the Age of the Jetsons: A Market Segmentation Analysis of Autonomous Ground Vehicles and Air Taxis in Five Large U.S. Cities," *AIAA Aviation 2020 Forum*, AIAA Paper 2020-3258, 2020. <https://doi.org/10.2514/6.2020-3258>
- [19] Hill, C., and Garrow, L. A., "A Market Segmentation Analysis for an eVTOL Air Taxi Shuttle," *AIAA Aviation 2021 Forum*, AIAA Paper 2021-3183, 2021. <https://doi.org/10.2514/6.2021-3183>
- [20] Fu, M., Rothfeld, R., and Antoniou, C., "Exploring Preferences for Transportation Modes in an Urban Air Mobility Environment: Munich Case Study," *Transportation Research Record*, Vol. 2673, No. 10, 2019, pp. 427–442. <https://doi.org/10.1177/0361198119843858>
- [21] Al Haddad, C., Chaniotakis, E., Straubinger, A., Plötner, K., and Antoniou, C., "Factors Affecting the Adoption and Use of Urban Air Mobility," *Transportation Research Part A: Policy and Practice*, Vol. 132, 2020, pp. 696–712, <https://www.sciencedirect.com/science/article/pii/S0965856419303830>. <https://doi.org/10.1016/j.tra.2019.12.020>

- [22] Roy, S., Kotwicz Herniczek, M. T., German, B. J., and Garrow, L. A., "User Base Estimation Methodology for a Business Airport Shuttle Air Taxi Service," *Journal of Air Transportation*, Vol. 29, No. 2, 2021, pp. 69–79.  
<https://doi.org/10.2514/1.D0216>
- [23] Bureau, U. C., "Longitudinal Employer-Household Dynamics," 2019,  
<https://lehd.ces.census.gov/data/#LODES>.
- [24] Bureau, U. C., "Census Data API: Income in the Past 12 Months," 2019,  
<https://api.census.gov/data/2019/ACS/ACS5/subject/groups/S1901.html>.
- [25] Bureau, U. C., "TIGER/Line Shapefiles," Section: Government, 2019,  
<https://www.census.gov/geographies/mapping-files/time-series/geo/tiger-line-file.html>.
- [26] Holden, J., and Goel, N., "Fast-Forwarding to a Future of On-Demand Urban Air Transportation," Uber Elevate TR, Oct. 2016,  
<https://www.uber.com/elevate.pdf/>.
- [27] Lim, E., and Hwang, H., "The Selection of Vertiport Location for On-Demand Mobility and Its Application to Seoul Metro Area," *International Journal of Aeronautical and Space Sciences*, Vol. 20, No. 1, 2019, pp. 260–272.  
<https://doi.org/10.1007/s42405-018-0117-0>
- [28] Daskilewicz, M., German, B., Warren, M., Garrow, L. A., Boddupalli, S.-S., and Douthat, T. H., "Progress in Vertiport Placement and Estimating Aircraft Range Requirements for eVTOL Daily Commuting," *2018 Aviation Technology, Integration, and Operations Conference*, AIAA Paper 2018-2884, 2018.  
<https://doi.org/10.2514/6.2018-2884>
- [29] Roy, S., Kotwicz Herniczek, M. T., Leonard, C., German, B. J., and Garrow, L. A., "Flight Scheduling and Fleet Sizing for an Airport Shuttle Air Taxi Service," *Journal of Air Transportation*, Vol. 30, No. 2, 2022, pp. 49–58.  
<https://doi.org/10.2514/1.D0265>
- [30] Kakwani, N. C., "Income Inequality and Poverty: Methods of Estimation and Policy Applications," The World Bank TR-10092, Washington, D.C., Jan. 1980.
- [31] Clementi, F., and Gallegati, M., "Pareto's Law of Income Distribution: Evidence for Germany, the United Kingdom, and the United States," *Econophysics of Wealth Distributions*, Springer, Berlin, 2005, pp. 3–14.  
[https://doi.org/10.1007/88-470-0389-X\\_1](https://doi.org/10.1007/88-470-0389-X_1)
- [32] Kitov, I., and Kitov, O., "The Dynamics of Personal Income Distribution and Inequality in the United States," *SSRN Electronic Journal*, Aug. 2013.  
<https://doi.org/10.2139/ssrn.2306463>
- [33] "UAM Concept of Operations," Federal Aviation Administration TR, Washington, D.C., 2020.
- [34] Kotwicz Herniczek, M. T., Yilmaz, E., Sanni, O., and German, B. J., "Drawing the Highways in the Sky for Urban Air Mobility Operations," *AIAA Aviation 2021 Forum*, AIAA Paper 2021-2376, 2021.  
<https://doi.org/10.2514/6.2021-2376>
- [35] Thippavong, D. P., Apaza, R., Barmore, B., Battiste, V., Burian, B., Dao, Q., Feary, M., Go, S., Goodrich, K. H., Homola, J., Idris, H. R., Kopardekar, P. H., Lachter, J. B., Neogi, N. A., Ng, H. K., Osegueda-Lohr, R. M., Patterson, M. D., and Verma, S. A., "Urban Air Mobility Airspace Integration Concepts and Considerations," *2018 Aviation Technology, Integration, and Operations Conference*, AIAA Paper 2018-3676, 2018.  
<https://doi.org/10.2514/6.2018-3676>
- [36] Bauranov, A., and Rakas, J., "Designing Airspace for Urban Air Mobility: A Review of Concepts and Approaches," *Progress in Aerospace Sciences*, Vol. 125, Aug. 2021, Paper 100726,  
<https://www.sciencedirect.com/science/article/pii/S0376042121000312>.  
<https://doi.org/10.1016/j.paerosci.2021.100726>
- [37] Luxen, D., and Vetter, C., "Real-Time Routing with OpenStreetMap Data," *Proceedings of the 19th ACM SIGSPATIAL International Conference on Advances in Geographic Information Systems*, ACM, New York, 2011, pp. 513–516.  
<https://doi.org/10.1145/2093973.2094062>
- [38] Skabardonis, A., and Dowling, R., "Improved Speed-Flow Relationships for Planning Applications," *Transportation Research Record: Journal of the Transportation Research Board*, Vol. 1572, No. 1, 1997, pp. 18–23.  
<https://doi.org/10.3141/1572-03>
- [39] Kerner, B. S., "Three-Phase Traffic Theory and Highway Capacity," *Physica A: Statistical Mechanics and Its Applications*, Vol. 333,
- Feb. 2004, pp. 379–440,  
<https://linkinghub.elsevier.com/retrieve/pii/S0378437103009221>.  
<https://doi.org/10.1016/j.physa.2003.10.017>
- [40] National Academies of Sciences, Engineering, and Medicine, *Highway Capacity Manual: Uninterrupted Flow*, 5th ed., Vol. 2, National Academies Press, Washington, D.C., 2010, Chap. 11.
- [41] Aghdashi, S., Roushail, N. M., Hajbabaie, A., and Schroeder, B. J., "Generic Speed-Flow Models for Basic Freeway Segments on General-Purpose and Managed Lanes in Undersaturated Flow Conditions," *Transportation Research Record: Journal of the Transportation Research Board*, Vol. 2483, No. 1, 2015, pp. 102–110.  
<https://doi.org/10.3141/2483-12>
- [42] National Academies of Sciences, Engineering, and Medicine, *Highway Capacity Manual: Interrupted Flow*, 5th ed., Vol. 3, National Academies Press, Washington, D.C., 2010, Chap. 17.
- [43] Ye, Q., Tarko, A., and Sinha, K. C., "Model of Free-Flow Speed for Indiana Arterial Roads," *Transportation Research Record: Journal of the Transportation Research Board*, Vol. 1776, No. 1, 2001, pp. 189–193.  
<https://doi.org/10.3141/1776-24>
- [44] Brilon, W., and Lohoff, J., "Speed-Flow Models for Freeways," *Procedia—Social and Behavioral Sciences*, Vol. 16, 2011, pp. 26–36,  
<https://linkinghub.elsevier.com/retrieve/pii/S1877042811009724>.  
<https://doi.org/10.1016/j.sbspro.2011.04.426>
- [45] Akçelik, R., "Travel Time Functions for Transport Planning Purposes: Davidson's Function, Its Time-Dependent Form and an Alternative Travel Time Function," *Australian Road Research*, Vol. 21, No. 3, 1991, pp. 49–59.
- [46] National Academies of Sciences, Engineering, and Medicine, *Highway Capacity Manual: A Guide for Multimodal Mobility Analysis*, 7th ed., Vol. 4, National Academies Press, Washington, D.C., 2022, Chap. 25.  
<https://doi.org/10.17226/26432>
- [47] "Highway Performance Monitoring System Field Manual," Federal Highway Administration TR-2125-0028, 2016,  
[https://www.fhwa.dot.gov/policyinformation/HPMS/fieldmanual/HPMS\\_field\\_manual\\_dec2016.pdf](https://www.fhwa.dot.gov/policyinformation/HPMS/fieldmanual/HPMS_field_manual_dec2016.pdf).
- [48] Chen, C.-C., and Knoblock, C. A., "Conflation of Geospatial Data," *Encyclopedia of GIS*, edited by S. Shekhar, and H. Xiong, Springer US, Boston, 2008, pp. 133–140.  
[https://doi.org/10.1007/978-0-387-35973-1\\_182](https://doi.org/10.1007/978-0-387-35973-1_182)
- [49] Garrow, L. A., German, B. J., and Leonard, C. E., "Urban Air Mobility: A Comprehensive Review and Comparative Analysis with Autonomous and Electric Ground Transportation for Informing Future Research," *Transportation Research Part C: Emerging Technologies*, Vol. 132, Nov. 2021, Paper 103377,  
<https://www.sciencedirect.com/science/article/pii/S0968090X21003788>.  
<https://doi.org/10.1016/j.trc.2021.103377>
- [50] "Revised Departmental Guidance on Valuation of Travel Time in Economic Analysis," U.S. Dept. of Transportation TR, Washington, D.C., Sept. 2016,  
[https://www.transportation.gov/sites/dot.gov/files/docs/2016\\_Revised\\_Value\\_of\\_Travel\\_Time\\_Guidance.pdf](https://www.transportation.gov/sites/dot.gov/files/docs/2016_Revised_Value_of_Travel_Time_Guidance.pdf).
- [51] "Your Driving Costs," American Automobile Association TR, 2021,  
<https://newsroom.aaa.com/wp-content/uploads/2021/08/2021-YDC-Brochure-Live.pdf>.
- [52] "Joby Aviation S4," Vertical Flight Society, 2022,  
<https://evtol.news/joby-s4>.
- [53] "Archer Midnight (Production Aircraft)," Vertical Flight Society, 2022,  
<https://evtol.news/archer>.
- [54] "Airworthiness Criteria for the Joby Aero, Inc. Model JAS4-1 Powered-Lift," 87 FR 67399, Federal Aviation Administration, Nov. 2022,  
<https://www.federalregister.gov/documents/2022/11/08/2022-23962/airworthiness-criteria-special-class-airworthiness-criteria-for-the-joby-aero-inc-model-jas4-1>.
- [55] "Airworthiness Criteria for the Archer Aviation Inc. Model M001 Powered-Lift," 87 FR 77749, Federal Aviation Administration, Dec. 2022,  
<https://www.federalregister.gov/documents/2022/12/20/2022-27445/airworthiness-criteria-special-class-airworthiness-criteria-for-the-archer-aviation-inc-model-m001>.